Low-Order Modeling of Can-Annular Combustors

Guillaume J. J. Fournier*
Technical University of Munich
Department of Mechanical Engineering
85748 Garching, Germany
e-mail: fournier@tfd.mw.tum.de

Max Meindl
Technical University of Munich
Department of Mechanical Engineering
85748 Garching, Germany
e-mail: meindl@tfd.mw.tum.de

Camilo F. Silva
Technical University of Munich
Department of Mechanical Engineering
85748 Garching, Germany
e-mail: silva@tfd.mw.tum.de

Giulio Ghirardo
Ansaldo Energia Switzerland
Haselstrasse 18
5400 Baden, Switzerland
e-mail: giulio.ghirardo@gmail.com

Mirko R. Bothien
Zurich University of Applied Sciences
Institute of Energy Systems and Fluid Engineering
8400 Winterthur, Switzerland
e-mail: mirko.bothien@zhaw.ch

Wolfgang Polifke
Technical University of Munich
Department of Mechanical Engineering
85748 Garching, Germany
e-mail: polifke@tum.de

*Address all correspondence to this author.

ABSTRACT

Heavy-duty land-based gas turbines are often designed with can-annular combustors, which consist of a set of identical cans, acoustically connected on the upstream side via the compressor plenum, and, downstream, with a small annular gap located at the transition with the first turbine stage. The modeling of this cross-talk area is crucial to predict the thermo-acoustic modes of the system. Thanks to the discrete rotational symmetry, Bloch wave theory can be exploited to reduce the system to a longitudinal combustor with a complex-valued equivalent outlet reflection coefficient, which models the annular gap. The present study reviews existing low-order models based purely on geometrical parameters and compares them to 2D Helmholtz simulations. We demonstrate that the modeling of the gap as a thin annulus is not suited for can-annular combustors and that the Rayleigh conductivity model only gives qualitative agreement. We then propose an extension for the equivalent reflection coefficient that accounts not only for geometrical but also flow parameters, by means of a characteristic length. The proposed model is in excellent agreement with 2D simulations and is able to correctly capture the eigenfrequencies of the system. We then perform a Design of Experiments study that allows us to explore various configurations and build correlations for the characteristic length. Finally, we discuss the validity limits of the proposed low-order modeling approach.

NOMENCLATURE

c $[\mathrm{m\,s^{-1}}]$ Speed of sound

f, g $[\mathrm{m\,s^{-1}}]$ Characteristic wave amplitudes

H $[\mathrm{m}]$ Width of the can

He [-] Helmholtz number, kL

k $[\mathrm{rad\,m^{-1}}]$ Wave number

K_R $[\mathrm{m}]$ Rayleigh conductivity

L $[\mathrm{m}]$ Length of the can

L_g $[\mathrm{m}]$ Width of the annular gap

$L_{char,\,m}$ $[\mathrm{m}]$ Characteristic length

L^* $[-]$ Aspect ratio of the can, L/H

L_g^* $[-]$ Coupling strength, L_g/H

$L^*_{char,\,m}$ $[-]$ Dimensionless characteristic length, $L_{char,\,m}/H$

m $[-]$ Bloch wave number

N $[-]$ Number of cans

p' [Pa] Acoustic pressure

$\mathcal{R}_m$ [$-$] Equivalent reflection coefficient

u' [$\mathrm{m\,s^{-1}}$] Acoustic velocity

φ [$\mathrm{m^2\,s^{-1}}$] Velocity potential

γ [$-$] Heat capacity ratio

ρ [$\mathrm{kg\,m^{-3}}$] Density

ω [$\mathrm{rad\,s^{-1}}$] Complex frequency

DoE Design of Experiments

LOM Low-Order Model

NRMSE Normalized Root-Mean-Square Error

INTRODUCTION

Can-annular combustors are commonly found in heavy-duty land-based gas turbines. In this application, N identical combustor cans are aligned along an annulus, hence the name. On the upstream side, the cans are acoustically connected to the compressor plenum. Downstream, a transition duct, as the name indicates, allows the cross-sectional area of the can to transform from a circular to an annular shape, in order to properly feed the turbine. Single can burners have often been considered to be a good approximation of the full system, since the combustion takes place in individual cans. However, a small annular gap is present just in front of the turbine inlet guide vanes, and this cross-talk area allows acoustic communication between neighboring cans. Recent studies showed that the can-to-can communication cannot be neglected when investigating thermoacoustic stability.

While annular combustors have been extensively studied in the last decades, can-annular configurations have received less attention. Bethke et al. [1] and Kaufmann et al. [2] were the first to numerically study can-annular configurations. They showed that accounting for the cross-talk area in a full system gives rise to new eigenmodes that were not observed in single can configurations. Panek et al. [3], based on experimental evidence and by means of a modal analysis, arrived at the same conclusion. Modes with mode shapes that involve multiple cans were observed for the full configuration but could not exist in a single can approximation. Farisco et al. [4] numerically investigated the effect of the geometry of the gap on the acoustic interaction between neighboring cans and showed that the cross-talk effect cannot be neglected. Ghirardo et al. [5] demonstrated numerically, by means of 2D Helmholtz simulations, and gave experimental evidence that modes of various azimuthal order arise due to the weak coupling between cans. It was shown that these modes come in ”clusters”, i.e. collections of several distinct modes with very close frequencies, but different growth rates.

Jegal et al. [6] and Moon et al. [7] experimentally investigated two adjacent burners connected with a cross-talk duct normal to the flow direction. They showed that the coupled system can exhibit strong oscillations, even if each single burner is stable when isolated. The oscillation patterns (axial and push-pull mode) have been observed to be strongly dependent on the equivalence ratio and on the geometrical location of the coupling duct. The work was extended to a configuration with four cans [8]. Because eigenmodes are closely-spaced and form clusters, the system can feature a mixed state with several distinct types of interaction patterns. The same test rig was used in [9] to analyze the effect of broken symmetry. It was shown that rotational asymmetry can lead to a variety of dynamic states (spinning azimuthal instabilities, mode localization, etc.) that are absent for the perfectly symmetric case, as discussed also by [5].

Recent studies tackled the problem at a more fundamental level by means of low-order network models. Using Bloch theory [10], the study of a can-annular system reduces to a single unit-cell. The behavior of the full system is preserved by accounting for all possible azimuthal orders. Von Saldern et al. [11] modeled the cross-talk communication between cans with the Rayleigh conductivity K_R. Using a simple constant K_R [12], they obtained an analytical model with only geometrical parameters, which was then used in a 1D network configuration to investigate the influence of the coupling strength on the clusters of thermoacoustic modes. In parallel, Fournier et al. [13] suggested that the modeling of annular combustors could be applied to can-annular configurations, where the gap is described by a thin annulus. The model was applied by Haeringer et al. [14] to propose a strategy to tune experimental single-can test-rigs to mimic the thermoacoustic behaviors of a full engine. Yoon [15] extended the model to account for mean flow and proposed a unified framework for both annular and can-annular combustors using a multi-input multi-output transfer function matrix.

In the present study, we want to investigate the validity of 1D models for can-annular combustors at a quantitative level by comparison of predictions with those of higher order models. We consider a 2D can-annular combustor, reduced to a single unit-cell with Bloch theory. We focus on the acoustic modeling of the cross-talk area. The paper is structured as follows: we first describe the dimensionless equivalent longitudinal network model. Then both the Rayleigh conductivity (RC) and the thin annulus (TA) models, which are based only on geometrical parameters, are compared to 2D Helmholtz reference simulations. We then propose an extension that accounts also for flow parameters, with a characteristic length, and demonstrate that such model can properly capture the eigenfrequencies. Finally, we perform a Design of Experiments study and propose correlations for the characteristic length. The limits of validity of the low-order model are discussed.

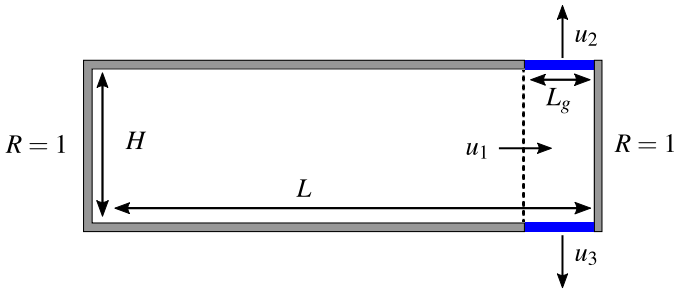

Fig. 1: Unit-cell of a generic can-annular combustor. The 3D geometry, as shown in Fig. 1 in [5], is approximated by a 2D can, of length L and width H, closed at the inlet and the outlet. Acoustic communication with the neighboring cans is possible through the cross-talk area of length L_g.

NETWORK MODEL OF A CAN-ANNULAR GEOMETRY WITH BLOCH BOUNDARY CONDITIONS

Case and Flow Description

A generic can-annular combustor consists of N identical cans, placed in an annular arrangement. Ghirardo et al. showed that a complex 3D geometry such as Fig. 1 in [5] can be well approximated by a 2D model. Following this approach, we consider here 2D cans of length L and of width H, as depicted in Fig. 1. Upstream, we neglect any possible influence of the plenum: the cans are decoupled and the reflection coefficient R_{in} is set to unity, following prior studies [5, 11]. On the downstream side, a high pressure turbine stage is placed to extract energy from the fluid. The acoustic response of such a turbine stage can be modeled by a reflection coefficient with a fixed gain lower than unity and a zero phase response [16]. In this study, we do not consider any loss mechanism and the outlet reflection coefficient is set to $R_{out} = 1$. Little quantitative change is expected when accounting for the losses [17]. The individual cans are acoustically coupled to each other through a small annular gap, of size L_g, located just upstream of the turbine.

In this study, we focus on the modeling of the acoustics of the set of transition pieces, where the Mach number is low, typically below 0.2 [3, 5]. Consequently, and similarly to axial combustors, the low Mach number assumption can be invoked by assuming zero mean flow when modeling the thermoacoustic behavior of cans, in particular wave propagation along the cans. Combustion is not taken into account because it occurs upstream of the considered domain. Accounting for it would lead to sections, inside the cans, with different temperatures and therefore different speed of sound, not to mention the influence of flame dynamics on the thermoacoustic modes. Since the combustion takes place significantly upstream of the turbine, the mean temperature can be assumed to be uniform in the region of the gap and the modeling approach remains valid. Therefore, the model proposed here can be used in future studies to investigate a more complete configuration. We also assume that mean quantities are constant and uniform over the entire domain. Finally, entropy waves are assumed to have a negligible effect and are not taken into account [5, 18].

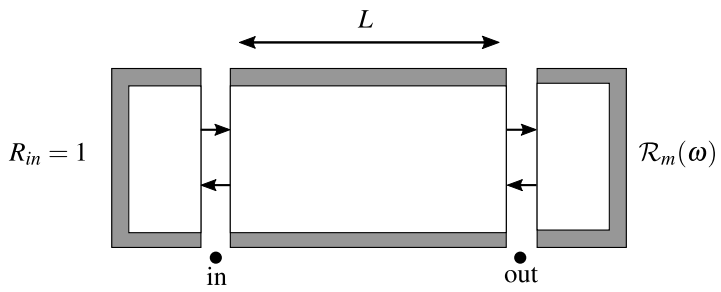

Fig. 2: Equivalent longitudinal network model of the unit-cell. The annular gap is modeled by the complex-valued reflection coefficient $\mathcal{R}_m(\omega)$, which depends on the frequency ω and the azimuthal order m.

Bloch-Wave Theory

The cans are geometrically identical, thus the system exhibits rotational symmetry. Bloch theory [10], which has been introduced in thermoacoustics by Mensah et al. [19] and is now well established [5, 13, 14, 20, 21], can then be applied. In the frequency domain, the acoustic pressure field can be written in the form:

$$\hat{p}\left(\boldsymbol{x}\right) = \psi\left(\boldsymbol{x}\right) e^{im\theta}, \;\; m = \begin{cases} -\dfrac{N}{2}+1, \ldots, \dfrac{N}{2} & N \text{ even} \\ -\dfrac{N-1}{2}, \ldots, \dfrac{N-1}{2} & N \text{ odd} \end{cases} \tag{1}$$

where θ is the azimuthal coordinate around the axis of discrete rotational symmetry, $\psi\left(\boldsymbol{x}\right)$ is a function identical in all unit cell and periodic in θ with a period $2\pi/N$, m is the Bloch wave number and we neglect to express the explicit dependence of $\hat{p}$ on frequency. Note that $\psi\left(\boldsymbol{x}\right)$ is not limited to a specific functional form, but can be any function that satisfies the aforementioned decomposition. The absolute value of m is identical to the azimuthal mode order [5].

The eigenmodes can be classified in three groups: axial ($m = 0$), push-pull ($m = N/2$) and degenerate pairs of spinning modes (all other values of m), which differ only by their spinning direction. From the study of a single unit-cell, the behavior of the full system can be assessed by considering all azimuthal mode orders m. In other words, we reduce our complete can-annular system to a single can where we apply Bloch boundaries in the region of the cross-talk, as depicted in Fig. 1.

Equivalent Longitudinal Network Model and Eigenvalue Problem

Low-order network models are well established for single can combustors [22–25] where, below the cut-on frequency of transverse modes, only acoustic plane waves propagate. The spatial extension of the gap is considered negligible compared to the wavelengths of interest meaning that the annular gap is acoustically compact. Therefore,

the unit-cell can be modeled by an acoustic network as shown in Fig. 2. The can is replaced by a simple duct of length L, closed at the upstream side $R_{in} = 1$. On the downstream end, the behavior of the can-to-can communication through the annular gap is modeled by the equivalent reflection coefficient $\mathcal{R}_m(\omega)$, which is, in general, frequency dependent. This longitudinal network model is equivalent to the full system as we can recover all the eigenmodes by varying the azimuthal mode order m hidden in the outlet boundary condition.

The governing equations describing this longitudinal network model involve the following parameters: the frequency ω, the speed of sound c, the length of the can L, the width of the can H, the length of the cross-talk area L_g. These five parameters admit a basis of two fundamental dimensions, time and distance. Following the Buckingham Π theorem [26], the system is fully described by only three dimensionless parameters. For consistency with prior studies, we choose the same as those introduced by Ghirardo et al. [5]. The first dimensionless parameter is the Helmholtz number $\mathrm{He} = kL$, where $k = \omega/c$ is the wave number, which represents a dimensionless frequency. Small values of He correspond to acoustic waves whose wavelength is acoustically compact compared to the can length L. The second is the coupling strength $L_g^* = L_g/H$. The third number $L^* = L/H$ is interpreted as the aspect ratio of the can.

In the context of network modeling, it is convenient to use Riemann invariants. We recall the definition of characteristic waves amplitudes

$$f \equiv \frac{1}{2}\left(\frac{p'}{\bar{\rho}c} + u'\right), \quad g \equiv \frac{1}{2}\left(\frac{p'}{\bar{\rho}c} - u'\right) \tag{2}$$

In the duct only plane waves propagate. The f and g waves at the cross-sections "in" and "out" of Fig. 2 are related as follows:

$$\begin{bmatrix} f_{out} \\ g_{out} \end{bmatrix} = \begin{bmatrix} e^{-i\omega\tau} & 0 \\ 0 & e^{i\omega\tau} \end{bmatrix} \begin{bmatrix} f_{in} \\ g_{in} \end{bmatrix} \tag{3}$$

The term $e^{-i\omega\tau}$ models the acoustic propagation of a plane wave, where $\tau = L/c$ is the time that takes an acoustic wave to cover the length L. The boundary conditions are given by

$$\begin{cases} g_{out} = \mathcal{R}_m(\omega) f_{out} \\ f_{in} = g_{in} \end{cases} \tag{4}$$

Inserting Eq. (4) into Eq. (3) and rewriting in terms of dimensionless parameters leads to the eigenvalue problem

$$\mathcal{R}_m(\mathrm{He})e^{-2i\mathrm{He}} = 1 \tag{5}$$

Equation (5) is complex-valued and thus gives conditions on the absolute value and the phase of the equivalent reflection coefficient $\mathcal{R}_m$. The first consequence is that $|\mathcal{R}_m(\mathrm{He})| = 1$. We considered a system with neither acoustic losses nor sources. It is therefore crucial to verify that the modeling approach does not introduce artificial losses or sources in the equivalent reflection coefficient $\mathcal{R}_m(\mathrm{He})$, i.e. its gain must be unity. The other consequence is that the eigenvalue problem reduces to a condition on the phase.

$$2\mathrm{He} - \angle\mathcal{R}_m(\mathrm{He}) \equiv 0 \mod 2\pi \tag{6}$$

where $\angle\mathcal{R}_m(\mathrm{He})$ denotes the argument of the equivalent reflection coefficient $\mathcal{R}_m(\mathrm{He})$. Note that, in general, Eq. (6) is non-linear in the Helmholtz number He and cannot be solved analytically.

2D REFERENCE CASE

In this section, we present the 2D Helmholtz case that serves as a reference for comparison with 1D low-order models. We choose the same parameters as in [5]: $N = 12$, $L^* = 2$, $L_g^* = 0.2$.

Numerical setup

The reference simulations for obtaining the reflection coefficient from the 2D Helmholtz equation are carried out with the commercial Finite Element solver Comsol Multiphysics. The parametrical setup of the geometry shown in Fig. 1 employs quadratic basis functions on a triangular mesh with cell sizes smaller than $10\,\mathrm{mm}$ to ensure grid independence. Boundary conditions for the sound hard walls, the non-reflecting inlet as well as the superposed acoustic forcing at the inlet are imposed weakly via the flux. The Bloch boundaries are enforced via Lagrange multiplier constraints. The Helmholtz equation for this case is then solved in the frequency domain in $10\,\mathrm{Hz}$ steps, up to the maximum frequency corresponding to $\mathrm{He} = \pi$.

Figure 3 presents the forced response of the can at the frequency $\mathrm{He} = \pi/2$, for the azimuthal order $m = 1$. From the inlet, only plane waves propagate but, as they approach the gap region, distortion is observed. In the cross-talk

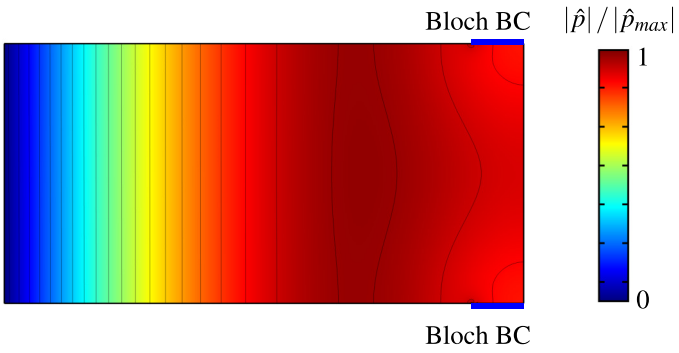

Fig. 3: Forced response of the system for the azimuthal order $m = 1$. The can is forced from the inlet with a wave f_{in} at the frequency He $= \pi/2$. Color indicates the normalized absolute pressure and black lines indicate isolines of pressure. Upstream of the can, plane waves propagate. Downstream, the gap introduces strong 2D effects that are not confined in the vicinity of the gap region but also extend upstream.

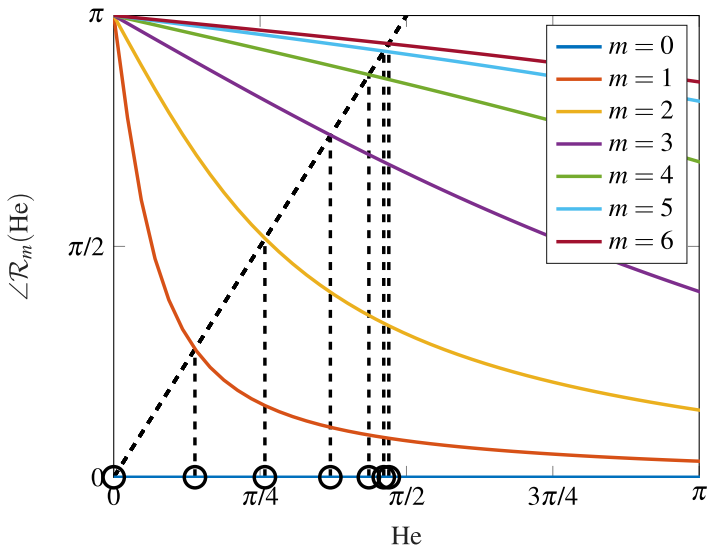

Fig. 4: Phase of the reflection coefficient $\mathcal{R}_{m,\,2D}$(He) of a set of $N = 12$ cans as a function of the dimensionless frequency He and the azimuthal order m of the forcing pattern. Circles, located at the intersection between the phase response and the line of equation 2He (black dashed line), indicate the eigenfrequencies of the whole set of cans. Eigenmodes of azimuthal orders $m = 4$, $m = 5$ and $m = 6$ have close frequencies, hence the denomination cluster.

area, the waves are not plane anymore and strong 2D effects are observed. These effects are not strictly confined in the vicinity of the gap but can also extend upstream, especially for higher azimuthal order. The results, in particular the reflection coefficients, are validated against those of Ghirardo et al. [5], which were obtained with an expansion on Chebyshev series of the 2D equations.

2D Equivalent Reflection Coefficients

The reflection coefficients $\mathcal{R}_{m,\,2D}(\mathrm{He})$ for an equivalent 1D geometry are obtained from 2D numerical simulations by computing the forced response of the set of cans at discrete frequencies and for each azimuthal order m. However, as seen in the previous section, strong 2D effects are present in the region of the gap, making any 1D post-processing at this location difficult. To overcome this limitation and to ensure reliable results, numerical measurements are performed at the inlet, upstream of the can, where the acoustics is closest to plane waves. In practice, for each azimuthal order m and for several discrete frequencies, we force the inlet with a wave f_{in} and measure the reflected wave g_{in}. From a 1D perspective, the measured ratio g_{in}/f_{in} is modeled as:

$$\frac{g_{in}}{f_{in}} = e^{-2i\mathrm{He}}\mathcal{R}_{m,\,2D}(\mathrm{He}) \tag{7}$$

The first term, $e^{-2i\mathrm{He}}$, represents the wave propagation in the duct from the inlet to the gap, and then again from the gap to the inlet, hence the factor of 2. $\mathcal{R}_{m,\,2D}(\mathrm{He})$ models the contribution of the annular gap.

From the 2D simulations, we computed the absolute value $|g_{in}/f_{in}|$ and verified that it is indeed unity. This result is expected: the waves cannot be amplified nor damped since no acoustic losses are taken into account and no energy is added to the system. On the other hand, the phase response is not trivial, and will especially depend on the azimuthal order of the mode, as reported in [5]. Although the equivalent reflection coefficient $\mathcal{R}_{m,\,2D}(\mathrm{He})$ cannot be directly assessed in the gap region, Eq. (7) can be rewritten:

$$\angle\mathcal{R}_{m,\,2D}(\mathrm{He}) = \angle\left(\frac{g_{in}}{f_{in}}\right) + 2\mathrm{He} \tag{8}$$

This post processing is useful because it allows us to keep only the behavior of the gap and remove the overemphasis of the contribution of the can (the phase shift due to the propagation in the can is much larger than the phase shift due to the gap, see Fig. 5 in [5]). Figure 4 shows the phase response of the equivalent reflection coefficient modeling the gap $\mathcal{R}_{m,\,2D}(\mathrm{He})$ as a function of the dimensionless frequency He, for all azimuthal mode orders m. For the axial mode $m = 0$, the phase is constant and equal to zero, meaning that $\mathcal{R}_{0,2D} = 1$. The gap has no influence on the axial mode and the can is simply exposed to the acoustic boundary induced by the turbine. For all other azimuthal order, the characteristics of the phase are not trivial and depend on the frequency. Starting from π in the low-frequency limit, it converges towards zero but the slope depends on the azimuthal order (low azimuthal orders go faster towards zero).

Another interesting feature of this representation is the possibility to directly read off the eigenvalues of the full system. Equation (6) can be rewritten:

$$\angle \mathcal{R}_m(\mathrm{He}) \equiv 2\mathrm{He} \mod 2\pi \tag{9}$$

Equation (9) indicates that the first set of eigenfrequencies is located at the intersection between the phase response and the straight line of equation 2He (black dotted line on Fig. 4). The second cluster, which consists of the harmonics of the modes of the first cluster, is located at the intersection with the line of equation $2\mathrm{He} - 2\pi$ (outside of the frequency range of Fig. 4) and so on for clusters of higher harmonics. Figure 4 shows that the eigenfrequencies of modes $m = 4$, $m = 5$ and $m = 6$ are really close, hence the denomination "cluster".

LOW-ORDER MODELS OF THE ANNULAR GAP BASED ON GEOMETRICAL PARAMETERS

In this section, we review the existing models proposed by von Saldern et al. [11] and Fournier et al. [13]. Both models are based on purely geometrical parameters and will be compared to the 2D Helmholtz simulations introduced in the previous section.

Rayleigh Conductivity model

The Rayleigh conductivity K_R of an aperture, defined as $K_R = i\omega\rho Q/\Delta p$, relates the volume flux Q through the aperture to the pressure difference Δp between the two sides [12]. It is the analogue of Ohm's law for 1D lumped acoustic systems. Von Saldern et al. [11] derived a 1D model of the gap where the Rayleigh conductivity K_R is used to relate the acoustic velocities inside the gap to the pressure gradient between cans, because $Q = A_{gap}u'$. The can was assumed to be circular, of radius r_{can}. In order to obtain a simple analytical expression, the gap was treated as a circular aperture. With this hypothesis, the Rayleigh conductivity is constant and relates to the gap radius as $K_R = 2r_{gap}$. Writing Eq. (10) from [11] with dimensionless parameters leads to

$$\mathcal{R}_{m,\,RC}(\mathrm{He}) = 1 - \frac{16\sin^2(\frac{\pi m}{N})}{i\mathrm{He}\frac{\pi}{2L^*\sqrt{L_g^*}} + 8\sin^2(\frac{\pi m}{N})} \tag{10}$$

In the rest of the paper we refer to it as the RC model, where RC stands for *Rayleigh conductivity*.

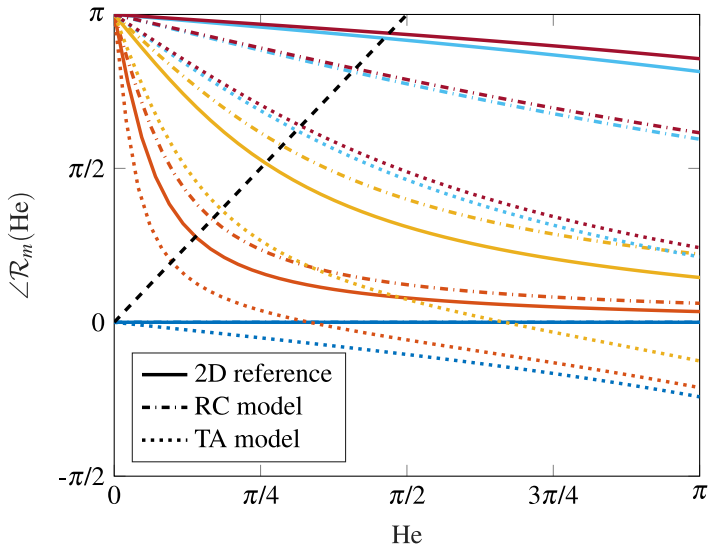

Fig. 5: Phase response of the annular gap as predicted by the Rayleigh conductivity model (dash-dot line) and thin annulus model (dotted line) compared to the 2D Helmholtz reference (full line). Colors indicate the azimuthal order as defined in Fig. 4. For each azimuthal order, the intersection of the phase response with the black dashed line gives the eigenfrequency. Both models are qualitatively correct in the low frequency limit. Nevertheless, they do not predict accurately the eigenfrequencies.

Thin Annulus model

Fournier et al. [13] proposed an alternative modeling strategy, where can-annular combustors are seen as limit cases of annular geometries: the cans are burner tubes of significant dimensions and the annular gap is an annular chamber where the axial spatial extension is negligible and the total azimuthal length corresponds to N times the width of a can. The annular gap is modeled as a thin annulus, i.e. a compact T-junction and ducts of lengths $H/2$ representing the width of the can. Following the results of Fournier et al., Eq. (14) in [13] can be written with dimensionless parameters:

$$\mathcal{R}_{m,\,TA}(\mathrm{He}) = 1 - \frac{4\cos\left(\frac{\mathrm{He}}{L^*}\right) - 4\cos\left(\frac{2\pi m}{N}\right)}{\frac{i}{L_g^*}\sin\left(\frac{\mathrm{He}}{L^*}\right) + 2\cos\left(\frac{\mathrm{He}}{L^*}\right) - 2\cos\left(\frac{2\pi m}{N}\right)} \tag{11}$$

In the following, we refer to it as the TA model, where TA stands for *thin annulus*.

Analysis of the low-order models

For a real-valued Helmholtz number He (marginally stable mode), it is straightforward to mathematically prove that $|\mathcal{R}_{m,\,RC}(\mathrm{He})| = |\mathcal{R}_{m,\,TA}(\mathrm{He})| = 1$. It follows that both models are satisfactory in the sense that they do not introduce spurious damping or amplification.

As reported in [5, 11, 13] and seen in the previous section, the phase response is non trivial. Figure 5 shows the phase response for both 1D models compared to the 2D Helmholtz reference case. For the sake of clarity, only the axial mode and modes of azimuthal order $m = 1, 2, 5, 6$ are represented. The first observation is that both models do not accurately reproduce the results of the 2D reference case: they do not provide quantitatively accurate results. For example, the TA model underpredicts the eigenfrequency of the first azimuthal order, whereas the RC model overpredicts it. The errors on the eigenfrequency are 29.3% and 20.7%, respectively. Similar behaviors are observed for the other azimuthal orders, and the error on the eigenvalue prediction varies from 11% to 35%. Akin results were observed by Yoon where the theoretical model, which can be seen as an extension of the TA model, always underpredicts the eigenfrequencies compared to FEM (Fig. 9 in [15]). Both RC and TA model underpredict the frequency at which the modes tend to cluster by 12.3% and 32.1% respectively.

Although being quantitatively inaccurate, the RC model exhibits a satisfactory qualitative behavior for the entire frequency range investigated. Starting from π, the phase decreases and converges asymptotically towards the horizontal zero line without crossing it. The axial mode is also well captured: the phase is constant and trivially zero. In contrast, the thin annulus (TA) model is not entirely satisfactory. For low frequencies, the TA model exhibits the correct qualitative behavior. This is explained by the fact that a Taylor expansion of Eq. (11) gives

$$\mathcal{R}_{m,\,TA}(\mathrm{He}) \approx 1 - \frac{8\sin^2(\frac{\pi m}{N})}{i\mathrm{He}\frac{1}{L^* L_g^*} + 4\sin^2(\frac{\pi m}{N})} \tag{12}$$

which is essentially the same structure as of the RC model (see Eq. (10)). However, as the frequency increases, for each mode order, the phase does not converge asymptotically towards the zero line but does cross it. These intersection points are located at the frequencies $\mathrm{He} = 2L^* m\pi/N$ and correspond to the passive acoustic mode of the thin annulus [13]. Therefore, for higher frequencies $\mathrm{He} \geq 2L^* m\pi/N$, the qualitative behavior is not satisfactory. We conclude that the cross-talk area of can-annular combustors should not be modeled as a thin annulus when considering higher frequencies. For the axial mode, the two ducts of the thin annulus that model the width of the can inherently add a non-negligible length to the total length of the can, hence the phase shift observed in Fig. 5. Note that this effect could be compensated but would require an individual tuning of the model for the axial mode.

In conclusion, the thin annulus assumption to model the gap in can-annular configurations is qualitatively valid only for low frequencies ($\mathrm{He} \leq 2L^* m\pi/N$). Conversely, the Rayleigh conductivity model gives the correct qualitative behavior over a wide frequency range. Nevertheless, because based purely on geometrical parameters, both models do not capture the correct phase response of the annular gap (see the error with the 2D reference on Fig. 5), and,

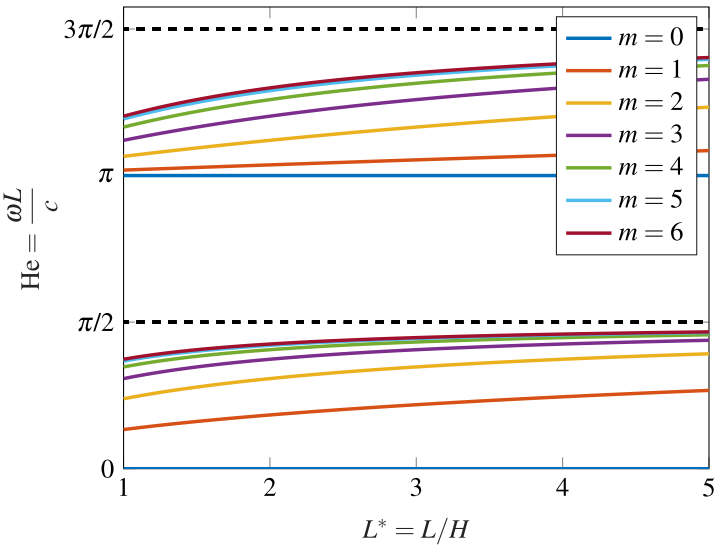

Fig. 6: Sensitivity of the first two eigenfrequencies as a function of the aspect ratio L^*. Small values of L^* correspond to a set of cans that are short compared to the circumference of the annular gap, that measures NH. Colors indicate the azimuthal order as defined in Fig. 4. When the length of the can becomes much larger than the other dimensions, the eigenmodes converge to the same solution, the quarter-wave mode and its harmonics. Modes with high azimuthal order converge faster and are closest within a cluster.

for all azimuthal orders, do not predict accurately the eigenfrequencies. These shortcomings motivate the need of an extension of the RC model to obtain quantitatively accurate results.

A few considerations on the spectrum structure and clusters

Although not suited for quantitative prediction, these simple models give good insight into the underlying physics. We consider two interesting limit cases.

- Case 1: L_g is zero. The gap is completely closed, i.e. the coupling strength is $L_g^* = 0$. The equivalent reflection coefficient becomes trivially $\mathcal{R}_{m,\,RC}(\mathrm{He}) = \mathcal{R}_{m,\,TA}(\mathrm{He}) = 1$: it is independent of the mode order and of the frequency. The gap closes and the annular configuration reduces to a purely longitudinal configuration where the outlet boundary condition is the choked exit. The eigenvalue problem becomes:

$$e^{-2i\mathrm{He}} = 1 \quad \Longrightarrow \quad \mathrm{He} = p\pi, \quad p \in \mathbb{N} \tag{13}$$

  which is the half-wave mode and its harmonics. In the limit case where the gap closes, all the modes of the first cluster collapse into one degenerate mode, the half-wave mode.

- Case 2: large aspect ratio. In the limit case where the length becomes much more significant than the width, i.e. $1/L^* \to 0$, the equivalent reflection coefficient is:

$$\mathcal{R}_{m,\,RC}(\mathrm{He}) \approx \mathcal{R}_{m,\,TA}(\mathrm{He}) \approx \begin{cases} 1, & m = 0 \\ -1, & m \neq 0 \end{cases} \tag{14}$$

The axial mode is unaffected by the annular gap and remains exposed to the choked outlet. The eigenmode associated is the half-wave mode $\mathrm{He} = 0$ and harmonics. On the other hand, all other azimuthal modes are now exposed to an open end ($R = -1$). The solutions of the eigenvalue problem are:

$$e^{-2i\mathrm{He}} = -1 \quad \Longrightarrow \quad \mathrm{He} = \frac{\pi}{2} + p\pi, \quad p \in \mathbb{N} \tag{15}$$

All the modes converge to the quarter-wave mode and its harmonics. This is physically explained by the fact that, in this limit case of long can, any phase shift introduced by the gap becomes negligible compared to the phase shift due to the propagation in the can itself. The effect of the azimuthal order on the outlet boundary becomes negligible, hence the outlet boundary is independent of the mode order and all modes converge to the same solution.

The phase of the equivalent reflection coefficient can be analytically determined:

$$\angle\mathcal{R}_{m,\,RC}(\mathrm{He}) = \pi - 2\arctan\left(\frac{\pi\mathrm{He}}{16L^*\sqrt{L_g^*}\sin^2(\frac{\pi m}{N})}\right) \tag{16}$$

This equation can be used to understand the spectrum structure. Recall that the eigenfrequency is located at the intersection with the straight line of equation 2He (Eq. (9)). When L^* increases, Eq. (16) shows that the phase response is less and less steep, the eigenfrequency is "pushed" to the right to higher frequencies, with the limit $\mathrm{He} = \pi/2$. Figure 6 presents the influence of the aspect ratio on the first two eigenfrequencies for all azimuthal orders. For a given azimuthal order m, when L^* increases, the eigenfrequency increases and converges towards the quarter-wave mode. Therefore, can-annular combustors with large aspect ratio L^* tend to have a more pronounced clustering effect. Similarly, for a given geometry (L^* and L_g^* fixed), when m increases, the phase response is less and less steep, the

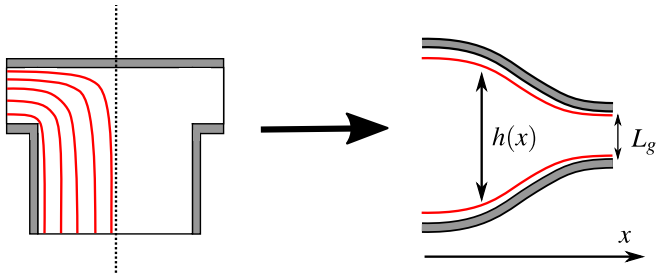

Fig. 7: Each half of the gap is treated as a 1D converging nozzle. $h(x)$ is the cross-section of the flow along the stream-path of the acoustic flow. The inertia of the volume of fluid is expressed in terms of a characteristic length $L_{char,\,m}$.

eigenmode is located at a higher frequency. That explains the spectrum structure: the higher the azimuthal order, the higher the eigenfrequency. Modes with higher azimuthal order will be the closest within a cluster. This sheds a new light when designing can-annular combustors: modes always come in clusters, outcome of a system that behaves as a collection of oscillators (cans) been weakly coupled (gap). The spread of the modes within a cluster depends on the system geometry (length of the can, gap design, etc.). This needs to be taken into account at the design stage as clusters of modes cannot be avoided. A related question arises: how should the combustor be designed to guarantee that all thermoacoustic modes are stable? This crucial and interesting question is beyond the scope of this study and will be left for future research.

LOW-ORDER MODEL BASED ON CHARACTERISTIC LENGTH

In this section we derive an extension for the reflection coefficient model that accounts not only for geometrical but also flow parameters. The gap is assumed to be acoustically compact. The mass conservation equation integrated over the control volume depicted in Fig. 1 reduces to conservation of volumetric flow rate:

$$Hu_1' - L_g u_2' - L_g u_3' = 0 \tag{17}$$

Equation (17) is rewritten with dimensionless parameters and Riemann invariants, which are more convenient to define a reflection coefficient.

$$\frac{1}{L_g^*}(f_1 - g_1) - (f_2 - g_2) - (f_3 - g_3) = 0 \tag{18}$$

Because of the rotational symmetry, we invoke Bloch theory to mutually connect location 2 and 3 with periodic Bloch boundaries [21].

$$\begin{cases} f_3 = g_2 e^{i\frac{2\pi m}{N}} & \text{(19a)} \\ g_3 = f_2 e^{i\frac{2\pi m}{N}} & \text{(19b)} \end{cases}$$

We define the equivalent reflection coefficient as $g_1 = \mathcal{R}_m f_1$. Using this definition and inserting Eq. (19) into Eq. (18) leads to

$$\frac{1}{L_g^*}(1-\mathcal{R}_m)f_1 + (e^{i\frac{2\pi m}{N}} - 1)f_2 + (1 - e^{i\frac{2\pi m}{N}})g_2 = 0 \tag{20}$$

Equation (20) has three unknowns, thus two more independent equations are required to close the problem. Note that for the axial mode $m = 0$, the equation directly reduces to $R_0(\text{He}) = 1$: the equivalent reflection coefficient is constant and is not affected by the cross-talk area.

We use the unsteady Bernoulli equation for irrotational homentropic flow [27].

$$0 = \frac{\partial}{\partial x}\left(\frac{\partial \varphi}{\partial t} + \frac{u^2}{2} + \frac{\gamma}{\gamma - 1}\frac{p}{\rho}\right) \tag{21}$$

where φ is the velocity potential and γ is the ratio of specific heat capacities (ideal gas behavior is implied). The equation is integrated along two streamlines of the mean flow, from location 1 to location 2 and from location 1 to location 3 respectively. It is possible to find a standing wave with a nodal line that coincides with the symmetry axis of the can in the considered unit-cell. This symmetry allows us to treat locations 2 and 3 similarly. We consider the integral in space of the first term of Eq. (21), the velocity potential.

$$\int_1^2 \frac{\partial}{\partial x}\left(\frac{\partial \varphi}{\partial t}\right)dx = \int_1^2 \frac{\partial}{\partial t}\left(\frac{\partial \varphi}{\partial x}\right)dx = \frac{\partial}{\partial t}\int_1^2 u(x)dx \tag{22}$$

As depicted in Fig. 7, from a 1D perspective, we consider the flow through the compact annular gap to be similar to the flow in a converging compact nozzle, which is a well established problem. Following prior studies for a compact

element with a varying cross-section [27–31], we define the characteristic length $L_{char,\,m}$

$$L_{char,\,m} = \int_1^2 \frac{u(x)}{u_2} dx \approx \int_1^2 \frac{L_g}{h(x)} dx \tag{23}$$

where $h(x)$ is the cross-section of the flow along the stream-path of the acoustic flow, and not the geometric cross-section across the element. For that reason, the characteristic length depends on the azimuthal order m. Physically, the characteristic length accounts for the inertia of the volume of fluid between the two reference positions. Assuming harmonic time-dependence, Equation (22) reduces to

$$\int_1^2 \frac{\partial}{\partial x_i}\left(\frac{\partial \varphi}{\partial t}\right) dx_i = i\omega L_{char,\,m} u_2 \tag{24}$$

The integral in space of the remaining two terms of Eq. (21) is simply evaluated at location 1 and 2. Linearization with Reynolds decomposition, assuming zero mean flow and neglecting higher order terms yields

$$ikL_{char,\,m} u_2' + \frac{p_2' - p_1'}{\bar{\rho} c} = 0 \tag{25}$$

where $k = \omega/c$ is the wavenumber. The integration from location 1 to 3 is done similarly. Switching to Riemann invariants, the problem can be cast into the homogeneous linear system of equations

$$\mathbf{M}(\mathrm{He}, m) \begin{bmatrix} f_1 \\ f_2 \\ g_2 \end{bmatrix} = \begin{bmatrix} 0 \\ 0 \\ 0 \end{bmatrix} \tag{26}$$

with the matrix $\mathbf{M}(\mathrm{He}, m)$ as

$$\underbrace{\begin{bmatrix} \frac{1-\mathcal{R}_m}{L_g^*} & e^{i\frac{2\pi m}{N}} - 1 & 1 - e^{i\frac{2\pi m}{N}} \\ -1-\mathcal{R}_m & 1 + ikL_{char,\,m} & 1 - ikL_{char,\,m} \\ -1-\mathcal{R}_m & e^{i\frac{2\pi m}{N}}(1 - ikL_{char,\,m}) & e^{i\frac{2\pi m}{N}}(1 + ikL_{char,\,m}) \end{bmatrix}}_{\mathbf{M}(\mathrm{He},m)} \tag{27}$$

The system shows non trivial solution if the determinant of $\mathbf{M}(\mathrm{He}, m)$ is null, which gives a condition for the reflection coefficient:

$$\mathcal{R}_{m,\,CL}(\mathrm{He}) = 1 - \frac{4\sin^2(\frac{\pi m}{N})}{i\mathrm{He}\frac{L^*_{char,\,m}}{L^* L_g^*} + 2\sin^2(\frac{\pi m}{N})} \tag{28}$$

where $L^*_{char,\,m} = L_{char,\,m}/H$ is the dimensionless characteristic length.

As shown by Schuermans et al. [32], the concept of effective length is interchangeable to the Rayleigh conductivity. Equation (28) is similar to Eq. (10) and can be seen as an extension of the RC model. However, the proposed model accounts not only for geometrical parameters but also for flow parameters with the inertial length $L_{char,\,m}$. In particular, the dependence of $L_{char,\,m}$ on the azimuthal order m reflects the fact that the acoustic flow is influenced by the azimuthal mode, hence the denomination flow parameter. Note that this is a purely acoustic perspective and it is not connected to mean flow, turbulence or similar features. The use of a characteristic length is well established and applicable to all sorts of elements, e.g. a premix burner [28], a sudden change in cross sectional area [30], an orifice [31], a nozzle [29], a Helmholtz resonator [33], among others. Note that we did not take into account the losses due to the abrupt changes in geometry. This consideration of losses is a natural extension of the present model and will be covered in future work.

The characteristic length $L_{char,\,m}$ can be determined from the 2D simulations using Eq. (22) or Eq. (23). However this post-processing can be tedious: it is not straight forward to determine an appropriate control volume, to extract a "characteristic" streamline representing the ensemble, to average the 2D quantities to compare with 1D, etc. Flohr et al. [31] proposed an alternative method to measure based on an analogy with the heat conduction equation but with a detrimental loss of accuracy. For the present case, we make use of the fact the reflection coefficient $\mathcal{R}_m$ numerically measured from the 2D simulations contains all the relevant information. In particular, $L_{char,\,m}$ is embedded in this

measurement as it directly shapes the the phase response of $\mathcal{R}_m$. As a result, $L_{char,\,m}$ becomes a physics-based parameter giving an additional degree of freedom. $L_{char,\,m}$ is assessed via an optimization problem by minimizing the normalized root mean squared error between the LOM and the numerical simulations, defined as

$$NRMSE = \frac{\sqrt{\frac{1}{n}\sum_{j=1}^{n}(y_j - \hat{y}_j)^2}}{\sigma} \tag{29}$$

where y_j is the phase response of the gap, obtained from numerical simulations, at the discrete frequency j, $\hat{y}_j$ the predicted value from the 1D model, n the number of frequency samples, and σ the standard deviation. Note that $L_{char,\,m}$ only depends on the azimuthal order m and is independent of frequency. Figure 8 presents the phase response of the annular gap as predicted by the characteristic length model compared to 2D Helmholtz simulations. For every azimuthal order, the low-order model shows excellent agreement with the 2D reference. The NRMSE between the LOM and the reference remains lower than 2.2%.

Since the phase response is properly modeled over the entire frequency range, it implies a correct eigenfrequency prediction. Table 1 shows, for every azimuthal mode, the eigenfrequency predicted by the characteristic length model and the relative error with the 2D reference. The maximal error observed is 2%, which is considered acceptable regarding all the assumptions and simplifications of the low-order model.

A simple 1D model, based on geometrical and flow parameters, is able to accurately model the cross-talk area of a can-annular combustor, despite the strong 2D effects observed at this location. These 2D effects are lumped into the equivalent length correction, as it is common in the acoustics literature. It is highlighted that, although changing with the mode order, the characteristic length $L_{char,\,m}$ does not depend on frequency. For each mode order, it is obtained from numerical simulations and valid for that case only. However, such low-order method is computationally inexpensive and may prove to be useful in concept and pre-design studies, where geometrical parameters are rapidly changing. In order to use it for new designs and ensure reliable results, one needs to determine how $L_{char,\,m}$ can be generalized.

GENERALIZATION OF THE MODEL TO CONFIGURATION WITH DIFFERENT GEOMETRICAL PARAMETERS

In this section, we investigate how the characteristic length $L_{char,\,m}$ can be generalized to other configurations. In particular, we analyze the influence of geometrical parameters.

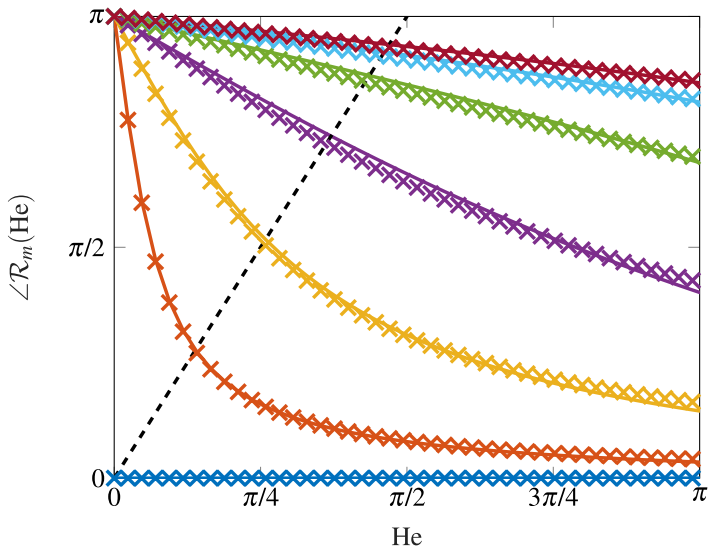

Fig. 8: Phase response of the annular gap as predicted by the characteristic length model (crosses) compared to the 2D Helmholtz reference (full line). Colors indicate the azimuthal order as defined in Fig. 4. For each azimuthal order, the intersection of the phase response with the black dashed line gives the eigenfrequency. The low-order model shows excellent agreement over the entire frequency range of interest compared to the 2D reference.

Table 1: Eigenfrequency prediction of the characteristic length model compared to the 2D Helmholtz reference for all azimuthal order.

	f_{2D} [Hz]	f_{CL} [Hz]	Error [%]
$m = 1$	58.98	58.73	0.4
$m = 2$	109.80	108.24	1.42
$m = 3$	157.35	154.14	2.03
$m = 4$	185.31	182.70	1.41
$m = 5$	196.12	194.63	0.76
$m = 6$	199.80	198.48	0.65

Design of Experiments Study

We perform a Design of Experiments (DoE) study [34] where the two dimensionless input parameters L^* and L_g^* vary in the range $[1 - 5]$ and $[0.1 - 0.3]$ respectively. These values correspond to realistic parameters for a gas turbine combustor. Following Loeppky et al. [35], who suggest that the sample size should be at least ten times the number of input parameters, the parameter space is filled by 40 points following a Latin Hypercube method, as shown in Fig. 9. For each set of parameters, a 2D Helmholtz simulation is performed and post-processed following the method described for the reference case.

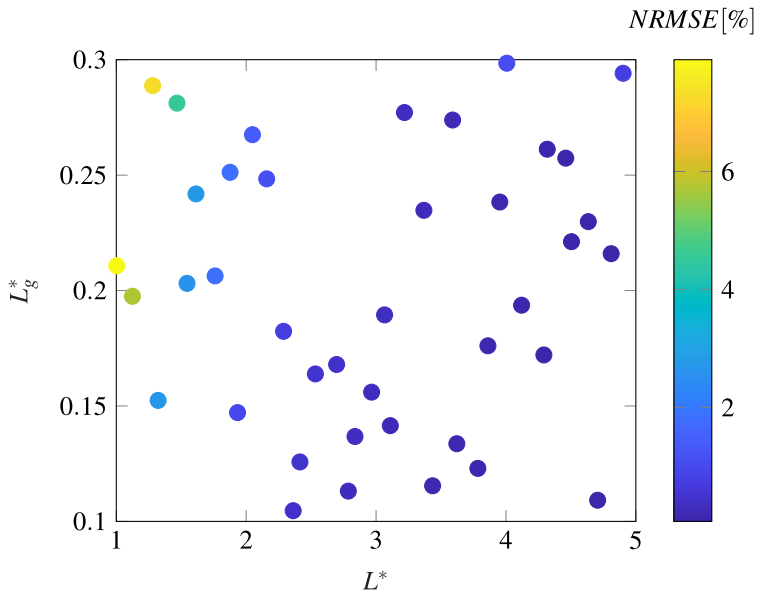

Fig. 9: Parameter space of the DoE filled by 40 points with a Latin Hypercube method. The color indicates the normalized root mean square error of the phase response between the low-order model and the 2D reference. For small aspect ratio L^* or for large coupling strength L_g^*, the error tends to increase.

Correlations for $L_{char,\,m}$

For each case, and for every azimuthal order, the characteristic length $L_{char,\,m}$ is determined. We excluded 4 data points that exhibited normalized root mean square errors between 2D and LOM greater than 5%, which was not considered acceptable. These larger errors, explained by the limits of validity of the LOM, are discussed later.

From a low-order network perspective, if we disregard the upstream can and consider only the gap itself, according to the Buckingham Π theorem [26], the latter can be modeled with only two parameters: a dimensionless frequency and the coupling strength L_g^*. But, as shown in the previous section, the characteristic length $L_{char,\,m}$ is independent of frequency. Therefore, from a 1D perspective, $L_{char,\,m}$ depends only on the coupling strength $L_g^* = L_g/H$. Figure 10 presents the normalized characteristic length $L^*_{char,\,m} = L_{char,\,m}/H$ as a function of the coupling strength L_g^*. For the sake of clarity, only mode order $m = 1$, $m = 3$ and $m = 6$ are shown. The color of the data points indicates the aspect ratio L^*. We can see that, for a coupling strength L_g^* from 10% to 30%, the normalized characteristic length $L^*_{char,\,m}$ scales linearly in the explored range. The coefficients of determination R^2 of the proposed linear regressions are 0.86, 0.77 and 0.93 respectively.

From the numerical simulations, for a given azimuthal order m, we observe that, for large values of L^*, the characteristic length can be considered independent of the aspect ratio L^* and is determined only by the coupling strength L_g^*. Indeed, from Fig. 10, we see that data points associated to configurations with similar coupling strength L_g^* but different aspect ratio L^* tend to be close to each other and the proposed correlations. On the other hand, the

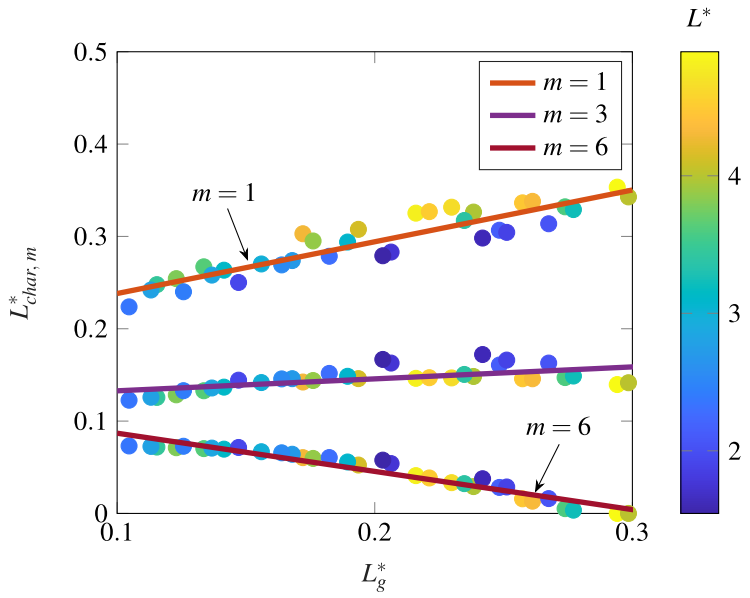

Fig. 10: Sensitivity of the normalized characteristic length $L^*_{char,\,m}$ as a function of the coupling strength L^*_g for azimuthal mode orders $m = 1$, $m = 3$ and $m = 6$. The color of the points indicates the aspect ratio of the can L^*, showing that the dependence of $L^*_{char,\,m}$ on L^* is weak in the studied range. In the explored range, $L^*_{char,\,m}$ scales linearly with the coupling strength L^*_g.

scatter is more pronounced for configuration with small aspect ratios: these points have the largest errors with the proposed linear regressions. Note also that, for these configurations, the error between 2D simulations and LOM when determining the characteristic length $L_{char,\,m}$ also tend to increase (recall Fig. 9). This is due to the limits of validity of the LOM approach, discussed in the last section. Considering the satisfactory linear regressions, it is reasonable to disregard the influence of the aspect ratio L^* and to consider the characteristic length $L_{char,\,m}$ primarily as a function of the azimuthal order m and the coupling strength $L^*_g = L_g/H$. In particular, for each mode order m, the linear regression gives:

$$L^*_{char,\,m} = a_{1,\,m} L^*_g + a_{0,\,m} \Longrightarrow L_{char,\,m} = a_{1,\,m} L_g + a_{0,\,m} H \tag{30}$$

It is highlighted that, as a first approximation, the characteristic length $L_{char,\,m}$ scales linearly with the gap size L_g and the width of the can H.

Depending on the coupling strength L^*_g and the azimuthal order m considered, the characteristic length can vary significantly. Physically, this is explained by the fact that an inertial length is strongly influenced by the contraction experienced by the flow. For example, it is common to observe a characteristic length much larger than the geometrical

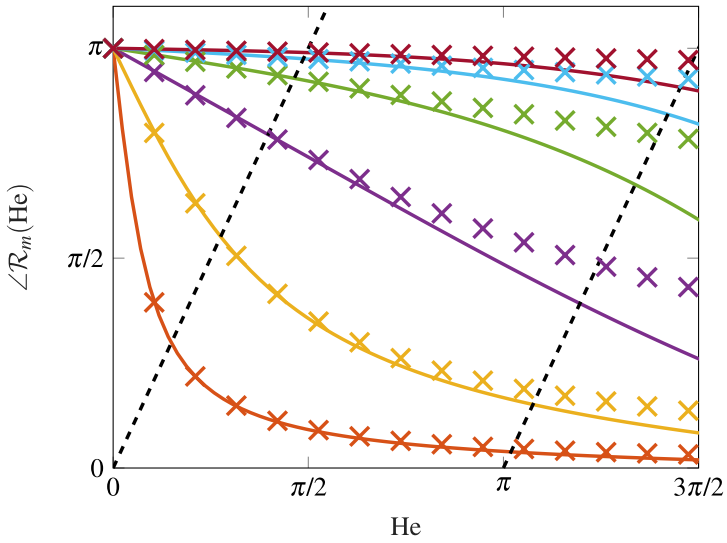

Fig. 11: Phase response of the gap as predicted by the characteristic length model (crosses) compared to the 2D Helmholtz reference (full line). Colors indicate the azimuthal order as defined in Fig. 4. Intersection with the black dashed lines gives the eigenfrequency. As the frequency increases, the gap becomes acoustically non-compact, the 1D modeling approach reaches its limits of validity and the model deviates from the reference case.

quantities of interest [27, 33]. For a given geometry, the characteristic length decreases with the azimuthal mode order, which is consistent with the fact that modes with higher azimuthal order exhibit a higher eigenfrequency, as explained previously. Finally, when the coupling strength increases, the relative importance of $L^*_{char,\,m}$ compared to L^*_g decreases towards zero, leading, for high values, to $\mathcal{R}_m \approx -1$. Indeed, if the coupling strength is large, i.e. if the gap size L_g is significant, the system can be seen as a can terminating in a large vessel, i.e. the can is exposed to an open end.

Limits of validity of the LOM approach

In the previous sections, we demonstrated that a low-order model based on a characteristic length can retrieve 2D results with a satisfying accuracy. In particular, the eigenfrequencies of the system are accurately predicted. However, such modeling approach has two limiting factors.

The first limitation comes from the assumption that, in the cans, only plane waves propagate and all other modes are said "cut-off". But as the frequency increases and reaches the cutoff frequency of a non-plane mode, that mode is no longer evanescent and can propagate: it is said cut-on. For example, for a circular can of radius $H/2$, the plane wave approximation remains valid up to the maximum frequency $\mathrm{He} < 2L^*\alpha_{11}$, where $\alpha_{11} \approx 1.84$ is the first zero of the Bessel function $J_1'(x)$ [36]. The maximum frequency is directly influenced by the aspect ratio of the can: for small aspect ratio L^*, the LOM will be able to accurately predict only the first cluster, whereas for large L^*, clusters

at higher frequencies, which consist of the harmonics of the mode of the first cluster, will also be correctly captured.

The second limitation comes from the hypothesis of an acoustically compact gap $kL_g \ll 1$, i.e. $\mathrm{He} \ll L^*/L_g^*$ with dimensionless parameters. Figure 11 shows the phase response of the characteristic length model compared to 2D simulations for $L^* = 2.05$ and $L_g^* = 0.27$. In the low frequency region, the LOM has a perfect agreement with numerical simulations. The first cluster (intersection with the first black dashed line) is captured accurately for every azimuthal order. However, as the frequency increases, the gap becomes non-compact. The LOM deviates from 2D reference and the second cluster is not captured at the correct frequencies. The error on the eigenfrequency prediction is around 6% for the second cluster, to put in perspective with an error of 1% or less for the first cluster. Although it might be considered still acceptable for the second cluster, note that it will be amplified for clusters at higher frequencies. It is therefore crucial, when considering clusters of higher harmonics, to verify that we remain within the domain of validity of our model.

SUMMARY AND CONCLUSION

In this paper, we investigated a generic can-annular combustor and focused on the acoustic modeling of the cross-talk area in front of the turbine that allows for can-to-can acoustic communication. We exploited the discrete rotational symmetry by using Bloch boundaries to reduce the combustor to a single unit-cell, while preserving the dynamics of the full system. We demonstrated that only three dimensionless parameters are required to model such configuration with a low-order network. The annular gap is replaced by a complex-valued equivalent reflection coefficient, which accounts for the azimuthal order of the mode.

We then reviewed two existing 1D models, based only on geometrical parameters, and compared them to a 2D Helmholtz reference. The first model describes the gap as a thin annulus. Although intuitive at first glance, this modeling approach is valid only in the low frequency limit and mainly suited for cans with large aspect ratios. The second model describes can-to-can communication with the Rayleigh conductivity. The qualitative behavior is satisfactory and valid for a wider frequency range. Both models can be used to understand the structure of the acoustic spectrum. However, they are based only on geometrical parameters and cannot predict, at a quantitative level, the correct eigenfrequencies of the system.

We then derived an extension that accounts not only for geometrical parameters, but also flow parameters in terms of an inertial characteristic length $L_{char,\,m}$. This additional parameter models how the acoustic flow in the gap is influenced by the azimuthal order of the mode. We demonstrated that such a 1D model can accurately capture the physics and shows excellent agreement with the reference, despite the strong 2D effects observed in the region of the gap.

We performed a Design of Experiments study to apply this model to other geometrical configuration and built correlations for $L_{char,\,m}$. We demonstrated that the characteristic length depends primarily on the azimuthal order m and the coupling strength L_g^* and linear regressions were proposed with satisfactory results. Finally, we discussed the limits of validity of the model.

In the present study, we considered a pure acoustic model. The impact of losses and mean flow on the characteristic length can be investigated in future work.

ACKNOWLEDGEMENTS

This project has received funding from the European Union's Horizon 2020 research and innovation programme under Grant Agreement No 765998 *Annular Instabilities and Transient Phenomena in Gas Turbine Combustors* (ANNULIGhT). Guillaume J. J. Fournier would like to thank Ansaldo Energia Switzerland for hosting him for this research. The authors would also like to thank Matthias Haeringer, Felix Schily and Shuai Guo for valuable discussions.

REFERENCES

[1] Bethke, S., Krebs, W., Flohr, P., and Prade, B., 2002. "Thermoacoustic properties of can annular combustors". In 8th AIAA/CEAS Aeroacoustics Conference & Exhibit, AIAA 2002-2570, p. 2570.

[2] Kaufmann, P., Krebs, W., Valdes, R., and Wever, U., 2008. "3D Thermoacoustic Properties of Single Can and Multi Can Combustor Configurations". In ASME Turbo Expo 2008: Power for Land, Sea, and Air, ASMEDC, pp. 527–538.

[3] Panek, L., Farisco, F., and Huth, M., 2017. "Thermo-Acoustic Characterization of Can-Can Interaction of a Can-Annular Combustion System Based on Unsteady CFD LES Simulation". In Proc 1st Global Power and Propulsion Forum, GPPF-2017-81, GPPS.

[4] Farisco, F., Panek, L., and Kok, J. B., 2017. "Thermo-acoustic cross-talk between cans in a can-annular combustor". *International Journal of Spray and Combustion Dynamics,* ***9***(4), Dec., pp. 452–469.

[5] Ghirardo, G., Di Giovine, C., Moeck, J. P., and Bothien, M. R., 2019. "Thermoacoustics of Can-Annular Combustors". *Journal of Engineering for Gas Turbines and Power,* ***141***(1), Jan., p. 011007.

[6] Jegal, H., Moon, K., Gu, J., Li, L. K., and Kim, K. T., 2019. "Mutual synchronization of two lean-premixed gas turbine combustors: Phase locking and amplitude death". *Combustion and Flame,* ***206***, Aug., pp. 424–437.

[7] Moon, K., Jegal, H., Gu, J., and Kim, K. T., 2019. "Combustion-acoustic interactions through cross-talk area between adjacent model gas turbine combustors". *Combustion and Flame,* ***202***, Apr., pp. 405–416.

[8] Moon, K., Jegal, H., Yoon, C., and Kim, K. T., 2020. "Cross-talk-interaction-induced combustion instabilities in a can-annular lean-premixed combustor configuration". *Combustion and Flame,* ***220***, Oct., pp. 178–188.

[9] Moon, K., Yoon, C., and Kim, K. T., 2021. "Influence of rotational asymmetry on thermoacoustic instabilities in a can-annular lean-premixed combustor". *Combustion and Flame,* ***223***, Jan., pp. 295–306.

[10] Bloch, F., 1929. "Über die Quantenmechanik der Elektronen in Kristallgittern". *Zeitschrift für Physik,* ***52***(7-8), July, pp. 555–600.

[11] von Saldern, J., Orchini, A., and Moeck, J., 2021. "Analysis of Thermoacoustic Modes in Can-Annular Combustors Using Effective Bloch-Type Boundary Conditions". *Journal of Engineering for Gas Turbines and Power,* ***143***(7), July, p. 071019.

[12] Howe, M. S., 1998. *Acoustics of Fluid-Structure Interactions*, first ed. Cambridge University Press, Aug.

[13] Fournier, G. J. J., Haeringer, M., Silva, C. F., and Polifke, W., 2021. "Low-Order Modeling to Investigate Clusters of Intrinsic Thermoacoustic Modes in Annular Combustors". *Journal of Engineering for Gas Turbines and Power,* ***143***(4), Apr., p. 041025.

[14] Haeringer, M., Fournier, G. J. J., Meindl, M., and Polifke, W., 2021. "A Strategy to Tune Acoustic Terminations of Single-Can Test-Rigs to Mimic Thermoacoustic Behavior of a Full Engine". *Journal of Engineering for Gas Turbines and Power,* ***143***(7), July, p. 710029.

[15] Yoon, M., 2021. "Thermoacoustics and combustion instability analysis for multi-burner combustors". *Journal of Sound and Vibration,* ***492***, Feb., p. 115774.

[16] Marble, F. E., and Candel, S. M., 1977. "Acoustic Disturbance from Gas Non-Uniformities Convected Through a Nozzle". *Journal of Sound and Vibration,* ***55***(2), Nov., pp. 225–243.

[17] Bauerheim, M., Duran, I., Livebardon, T., Wang, G., Moreau, S., and Poinsot, T., 2016. "Transmission and reflection of acoustic and entropy waves through a stator–rotor stage". *Journal of Sound and Vibration,* ***374***, pp. 260–278.

[18] Morgans, A. S., and Duran, I., 2016. "Entropy Noise: A Review of Theory, Progress and Challenges". *International Journal of Spray and Combustion Dynamics,* ***8***(4), pp. 285–298.

[19] Mensah, G. A., Campa, G., and Moeck, J. P., 2016. "Efficient Computation of Thermoacoustic Modes in Industrial Annular Combustion Chambers Based on Bloch-Wave Theory". *Journal of Engineering for Gas Turbines and Power,* ***138***(8), Aug., p. 081502.

[20] Ghirardo, G., Moeck, J. P., and Bothien, M. R., 2020. "Effect of Noise and Nonlinearities on Thermoacoustics of Can-Annular Combustors". *Journal of Engineering for Gas Turbines and Power,* ***142***(4), Apr., p. 041005.

[21] Haeringer, M., and Polifke, W., 2019. "Time Domain Bloch Boundary Conditions for Efficient Simulation of

Thermoacoustic Limit-Cycles in (Can-)Annular Combustors". *Journal of Engineering for Gas Turbines and Power,* ***141***(12), p. 121005.

[22] Dowling, A. P., and Stow, S. R., 2003. "Acoustic Analysis of Gas Turbine Combustors". *Journal of Propulsion and Power,* ***19***(5), pp. 751–764.

[23] Schuermans, B., Bellucci, V., and Paschereit, C. O., 2003. "Thermoacoustic Modeling and Control of Multi-Burner Combustion Systems". In Proceedings of the ASME Turbo Expo 2003, Collocated with the 2003 International Joint Power Generation Conference, GT2003-38688, ASME, pp. 509–519.

[24] Bothien, M., Moeck, J., Lacarelle, A., and Paschereit, C. O., 2007. "Time Domain Modelling and Stability Analysis of Complex Thermoacoustic Systems". *Proceedings of the Institution of Mechanical Engineers, Part A: Journal of Power and Energy,* ***221***(5), Jan., pp. 657–668.

[25] Emmert, T., Meindl, M., Jaensch, S., and Polifke, W., 2016. "Linear State Space Interconnect Modeling of Acoustic Systems". *Acta Acustica united with Acustica,* ***102***(5), pp. 824–833.

[26] Barenblatt, G. I., 2003. *Scaling*. Cambridge Texts in Applied Mathematics. Cambridge University Press, Cambridge.

[27] Polifke, W., 2004. "Combustion Instabilities". In *Advances in Aeroacoustics and Applications*, J. Anthoine and A. Hirschberg, eds., VKI LS 2004-05. Von Karman Institute, Rhode-St-Genèse, BE.

[28] Paschereit, C. O., and Polifke, W., 1998. "Investigation of the Thermo-Acoustic Characteristics of a Lean Premixed Gas Turbine Burner". In Int'l Gas Turbine and Aeroengine Congress & Exposition, ASME 98-GT-582, ASME.

[29] Stow, S., Dowling, A., and Hynes, T., 2002. "Reflection of Circumferential Modes in a Choked Nozzle". *Journal of Fluid Mechanics,* ***467***, pp. 215–239.

[30] Gentemann, A., Fischer, A., Evesque, S., and Polifke, W., 2003. "Acoustic Transfer Matrix Reconstruction and Analysis for Ducts with Sudden Change of Area". In 9th AIAA/CEAS Aeroacoustics Conference, AIAA-2003-3142, AIAA, pp. 11–11.

[31] Flohr, P., Paschereit, C. O., and Bellucci, V., 2003. "Steady CFD Analysis for Gas Turbine Burner Transfer Functions". In 41st AIAA Aerospace Sciences Meeting & Exhibit, AIAA, pp. 11–11.

[32] Schuermans, B., Bellucci, V., Guethe, F., Meili, F., Flohr, P., and Paschereit, O., 2004. "A Detailed Analysis of Thermoacoustic Interaction Mechanisms in a Turbulent Premixed Flame". In Int'l Gas Turbine and Aeroengine Congress & Exposition, GT2004-53831, ASME.

[33] Bothien, M. R., and Wassmer, D., 2015. "Impact of Density Discontinuities on the Resonance Frequency of Helmholtz Resonators". *AIAA Journal,* ***53***(4), pp. 877–887.

[34] McClarren, R., 2018. *Uncertainty Quantification and Predictive Computational Science: A Foundation for Physical Scientists and Engineers*. Springer International Publishing.

[35] Loeppky, J. L., Sacks, J., and Welch, W. J., 2009. "Choosing the Sample Size of a Computer Experiment: A Practical Guide". *Technometrics,* ***51***(4), Nov., pp. 366–376.

[36] Munjal, M. L., 2014. *Acoustics of Ducts and Mufflers*, second ed. Wiley, Chichester, West Sussex, United Kingdom.